Phase Locking Dynamics in 2D Josephson Junction Networks with Small Loop Inductances

Wolfram Krech, Michael Basler, Birgit Frank, and Konstantin Yu. Platov
Friedrich Schiller University, Institute of Solid State Physics, Helmholtzweg 5, D-07743 Jena, Germany

***Abstract*—We discuss some theoretical problems in connection with external flux in hybrid 2D Josephson networks with junctions attached to the lines in bias direction only. With very small loop inductances assumed, the junctions within the interferometer configurations perpendicular to the bias current are strongly coupled. This way the synchronization of the Josephson oscillations in 2D hybrid arrays reveals a certain similarity to the well-known phase locking dynamics in linear Josephson junction chains.**

We start with an analysis of phase locking in simple SQUID cells within the resistively shunted junction (RSJ) model. Taking into account the flux quantization, we develop a systematic perturbation method to investigate the dynamics of cells with small but non-vanishing loop inductances. These strongly coupled SQUIDs possess quasi-uniform synchronization with very small phase shifts between the junctions' oscillating voltages for allmost all values of external flux. Next, we consider the mutual phase locking in arrays consisting of small-inductance loops coupled via a joint line transverse to the bias current. It is shown that in the stable dynamic regime both cells oscillate in an antiphase mode.

Based on the analytical procedure combining ideas from small-inductance approximation with those from slowly varying phase we deduce rigorous results for ladder arrays and inductively coupled multi-junction interferometers. Finally, considering hybrid Josephson junction networks with external load impedance and solving the problem of interplay of long-range and nearest-neighbour interactions, we demonstrate a possibility to look for effective multi-junction microwave radiation sources systematically.

I. Introduction

Discrete Josephson junction arrays have been under consideration as tunable millimetre and sub-mm wavelength radiation sources for several years now [1]–[3]. A growing interest has evolved in 2D arrays [4]–[9] because they should be capable of delivering a larger radiation out-

Manuscript received August 31, 2000.
E-mail address of W. Krech (corr. author): owk@rz.uni-jena.de.
This work was supported in part by the Deutsche Forschungsgemeinschaft under Grant No. KR 1172/4-1,2.

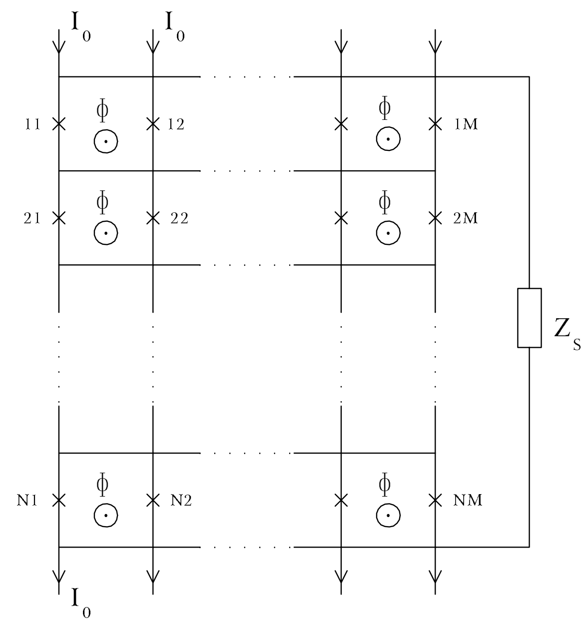

Fig. 1. The hybrid Josephson junction array under consideration. The 2D network consists of N interferometer rows and M columns shunted by an external load impedance Z_s. Loop inductances are not marked, I_0 is the bias current per column.

put and substantially decreasing the oscillation linewidth compared to their 1D counterparts. In particular, in this paper we are concerned with hybrid networks containing $N \times M$ junctions attached to the lines in bias direction only (Fig. 1). In order to draw a picture of the mentioned advantages of networks, we call to mind the optimum oscillation power P_{opt} which can be delivered to a matched load by a linear chain of $N \times 1$ junctions. With sufficiently high frequencies assumed, $\nu \gtrsim \nu_c = I_c R_n/\Phi_0$ ($I_0 \gtrsim 1.5 I_c$), this is within the frame of the RSJ model [10]

$$P_{opt}^{(N\times 1)} = \frac{1}{8} I_c^2 R_s, \tag{1}$$

where the impedance match is achieved by optimizing the number of junctions,

$$N = N_{opt} = R_s/R_n. \tag{2}$$

I_c and R_n are the critical current and normal resistance of the (identical) junctions, respectively. Otherwise, if

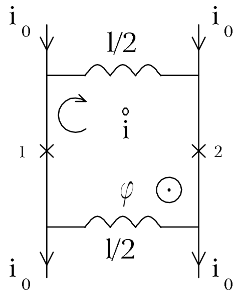

Fig. 2. The SQUID cell which can be described with the strong-coupling method. The symbols l, φ, and i° explained in the text denote scaled loop inductance, flux through the SQUID ring, and circular current, respectively.

only fluctuations due to thermal noise are considered, the linewidth $\Delta\nu$ is [10]

$$\Delta\nu^{(N\times 1)} = \frac{1}{N}\frac{4\pi}{\Phi_0^2} R_n k_B T. \quad (3)$$

Introducing the substitutions (cf. [3])

$$I_c \to M I_c, \quad R_n \to R_n/M, \quad (4)$$

the relations (1)-(3) are easily generalized to arrive at the corresponding expressions

$$P_{opt}^{(N\times M)} = \frac{1}{8} I_c^2 R_s, \quad (5)$$

$$\Delta\nu^{(N\times M)} = \frac{1}{NM}\frac{4\pi}{\Phi_0^2} R_n k_B T \quad (6)$$

with

$$N = N_{opt} = M R_s / R_n \quad (7)$$

for arrays with N rows and M columns. However, the scaling (4) is only true if all junctions are unifomly phase-locked. But the dynamical behaviour of such arrays is rather complicated, especially, the influence of external magnetic flux is not yet completely understood [11], [12]. The presence of a magnetic field can cause certain complications, e.g. the coexistence of in-phase and antiphase coherent states [13]. The values of the loop inductances play a crucial role in these processes and in synchronization dynamics in general. In order to illustrate this fact, we consider a simple SQUID cell (Fig. 2) with weak coupling [10], [14], i.e.,

$$l \equiv 2\pi I_c L/\Phi_0 \gg 1. \quad (8)$$

(l marks the normalized loop inductance.) In this case, coupling can be neglected in zeroth order with respect to l^{-1}, and both junctions oscillate with the respective phases of over-critically biased free junctions,

$$\Phi_{1,2} = 2\arctan\left[\frac{\zeta_0}{\zeta_0+1}\tan\left(\frac{\zeta_0 s - \delta_{1,2}}{2}\right)\right] + \frac{\pi}{2}, \quad (9)$$

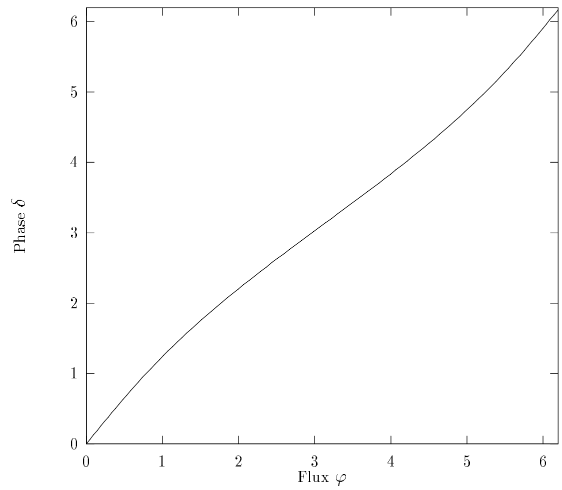

Fig. 3. Voltage phase shift δ vs. normalized external flux from analytical approximation for weak inductive coupling, $l \gg 1$ (bias current $i_0 = 1.5$).

showing an oscillation frequency

$$\zeta_0 = (i_0^2 - 1)^{1/2} \quad (10)$$

and constant phases δ_1 and δ_2. For the sake of simplicity, we have introduced the normalized bias current,

$$i_0 = I_0/I_c, \quad (11)$$

which is supposed to fulfill the condition $i_0 > 1$ here. s denotes the scaled time,

$$s = \frac{2e}{\hbar} I_c R_n t. \quad (12)$$

Furthermore, we define the normalized external flux through the SQUID loop,

$$\varphi = 2\pi\Phi/\Phi_0. \quad (13)$$

Looking for lowest-order phase locking solutions [10], [14], [15],

$$\dot{\delta} = 0, \quad \delta = \delta_1 - \delta_2, \quad (14)$$

one finds

$$\delta - \frac{1}{i_0(1_0 + \zeta_0)}\sin\delta = \varphi. \quad (15)$$

(The dot ($\dot{}$) means differentiation with respect to the dimensionless time s (12).) For usual operation regimes with $i_0 \simeq 1.5$ this results in an approximately linear relation between δ and φ, as indicated in Fig. 3. This way 2D networks, in contrast to 1D series arrays, suffer in case of $l > 1$ from a high sensitivity to magnetic fields because of their intrinsic superconducting loops representing multi-junction dc SQUIDs. The pronounced dependence (15) of the mutual phase shift δ on the flux φ may ultimately explain the fact why, up to now, the radiation power of

2D arrays [16], [17] was found to be much smaller than that of 1D arrays [6], [18].

In order to simplify the dynamics of 2D networks in general, the nonvanishing inductance of the loops should be minimized, $l \ll 1$. To investigate this conception with respect to its consequences, we perform within the RSJ model a theoretical analysis of phase locking in strongly coupled Josephson junction cells (Sec. II). For this purpose, we develop a systematic perturbation method allowing the investigation of phase locking in cells with small loop inductance. In Sec. III, we consider synchronization in a simple 2D array consisting of two loops coupled via an inductive joint line transverse to the bias current. It is shown that in the stable oscillation regime both cells oscillate in an antiphase mode. This result is applied to a study of externally loaded Josephson junction ladder arrays (Sec. IV). Here a Lyapunov stability condition is found controlling the realization of the radiating uniform oscillation regime.

Based on the analytical procedure combining ideas from small-inductance approximation with those from slowly varying phase, we deduce rigorous results on inductively coupled multi-junction interferometers (Sec. V). Finally, after solving the problem of interplay of long-range and nearest-neighbour interferometer interactions, we propose effectively operating microwave radiation sources based on hybrid Josephson junction networks with small loop inductances in Sec. VI.

II. Phase locking in strongly coupled SQUID cells

Contrary to most theoretical investigations, which are mainly based on computer simulations, we concentrate on approximate analytical results. For the sake of simplicity, the required calculations are performed by means of common normalized variables (cf. Sec. I). The advantage of this designation is usually a better insight into physical mechanisms in combination with a broader range of applicability concerning the choice of parameters. However, we find it quite valuable to compare analytical predictions with numerical results occasionally.

The Josephson dynamics of the SQUID-like cell with identical junctions shown in Fig. 2 is described by the basic equations

$$\dot{\Phi}_k + \sin \Phi_k = i_k \quad (k = 1, 2) \tag{16}$$

of the RSJ model in conjunction with conservation of current,

$$2 i_0 = i_1 + i_2, \tag{17}$$

and flux quantization,

$$\Phi_2 - \Phi_1 - \varphi + l i^\circ = 0. \tag{18}$$

Here the circular current is defined as

$$i^\circ = i_2 - i_1. \tag{19}$$

A. Perturbation scheme for strong inductive coupling

We find it convenient to introduce new variables,

$$\Sigma = (\Phi_2 + \Phi_1)/2, \quad \Delta = (\Phi_2 - \Phi_1)/2, \tag{20}$$

providing the set of equations

$$\dot{\Sigma} + \sin \Sigma \cos \Delta = i_0, \tag{21}$$

$$\dot{\Delta} + \cos \Sigma \sin \Delta = \frac{1}{l}(\varphi - 2\Delta). \tag{22}$$

These equations already indicate that the behaviour of Σ is necessarily determined by the bias current i_0 and that of Δ by the flux φ. We perform a perturbation expansion valid for small coupling, $l \ll 1$,

$$\Sigma = \Sigma_0 + l\Sigma_1 + \cdots, \tag{23}$$

$$\Delta = \Delta_0 + l\Delta_1 + \cdots. \tag{24}$$

Expanding Eqs. (21,22) and balancing equal orders of l, we arrive at the following set of relations [15], [19]:

$$\dot{\Sigma}_0 + \sin \Sigma_0 \cos \Delta_0 = i_0, \tag{25}$$

$$\dot{\Sigma}_1 + \Sigma_1 \cos \Sigma_0 \cos \Delta_0 - \Delta_1 \sin \Sigma_0 \sin \Delta_0 = 0, \tag{26}$$

$$2\Delta_0 = \varphi, \tag{27}$$

$$\dot{\Delta}_0 + \cos \Sigma_0 \sin \Delta_0 = -2\Delta_1. \tag{28}$$

At first, solving the simpler lowest-order Eqs. (25,27) and exploiting their results, we obtain, after a lengthy calculation, the complete solution scheme

$$\Sigma_0 = 2 \arctan \left(\frac{\zeta_0}{i_0 + \cos \frac{\varphi}{2}} \tan \frac{\zeta_0 s}{2} \right) + \frac{\pi}{2}, \tag{29}$$

$$\Delta_0 = \frac{\varphi}{2}, \tag{30}$$

$$\Sigma_1 = \frac{\tan^2 \frac{\varphi}{2}}{2(i_0 + \cos \frac{\varphi}{2} \cos \zeta_0 s)} \left[i_0 \cos \frac{\varphi}{2}(1 - \cos \zeta_0 s) + \zeta_0^2 \ln \frac{i_0 + \cos \frac{\varphi}{2} \cos \zeta_0 s}{i_0 + \cos \frac{\varphi}{2}} \right], \tag{31}$$

$$\Delta_1 = \frac{1}{2} \sin \frac{\varphi}{2} \frac{\zeta_0 \sin \zeta_0 s}{i_0 + \cos \frac{\varphi}{2} \cos \zeta_0 s} \tag{32}$$

with the re-definition of the frequency expression (10),

$$\zeta_0 = \left(i_0^2 - \cos^2 \frac{\varphi}{2} \right)^{1/2}, \tag{33}$$

suggested by the critical SQUID current, $c(\varphi) = \cos \frac{\varphi}{2}$. After solving the equations for Σ and Δ up to the first order, we can go back to the Josephson phases and, finally, determine voltages across junctions,

$$v_{1,2} = \dot{\Phi}_{1,2} = \dot{\Sigma} \pm \dot{\Delta}. \tag{34}$$

This result has several interesting features. First, for any φ there exists a (stable) solution exhibiting phase locking. Second, the oscillation frequency becomes flux-dependent, which may cause serious consequences for synchronization in larger arrays. Third, there is a phase shift between junction voltage oscillations caused by the last term in Eq. (34) in general.

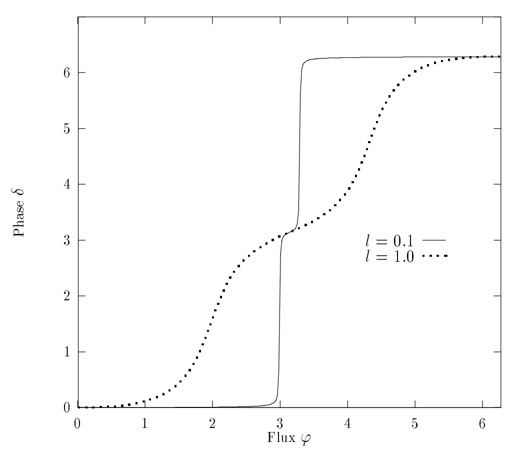

Fig. 4. Phase shift δ vs. normalized external flux φ for strong inductive coupling ($l = 0.1$) and medium inductive coupling ($l = 1.0$) obtained from analytical approximation ($i_0 = 1.5$).

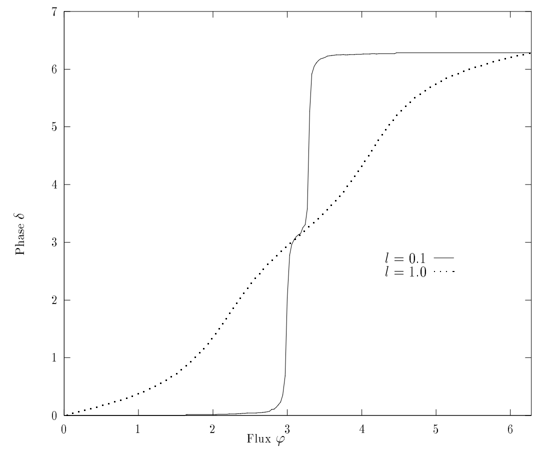

Fig. 5. Like Fig. 4, results obtained from numerical simulation.

B. Evaluation of phase shift

In general, there is no simple definition of phase shift in cases like this, because of higher harmonics present in the solution. A plausible approach is to define phase shift based on the lowest harmonics. For this purpose, we have to evaluate the first coefficients of the Fourier series

$$\dot{\Phi}_{1,2} = \alpha + a_{1,2}\cos\zeta_0 s + b_{1,2}\sin\zeta_0 s + \cdots. \qquad (35)$$

After a tedious calculation involving an expansion of a logarithmic term (cf. (31)) we arrive at

$$\alpha = \zeta_0, \qquad (36)$$

$$a_{1,2} = \frac{\zeta_0}{i_0+\zeta_0}\left(-2\cos\frac{\varphi}{2} \mp \zeta_0\sin\frac{\varphi}{2}\right), \qquad (37)$$

$$\begin{aligned} b_{1,2} &= b \\ &= l\frac{\sin^2\frac{\varphi}{2}\cos\frac{\varphi}{2}}{i_0+\zeta_0}\left[1+\frac{\cos\frac{\varphi}{2}}{i_0}+\frac{\zeta_0^3}{4i_0^2(i_0+\zeta_0)}\right]. \end{aligned} \qquad (38)$$

With these coefficients known, we can work out the phase shift between the voltage oscillations,

$$\begin{aligned} \delta &= \mathrm{sgn}[b(a_1-a_2)] \times \\ &\times\left[\pi - \arccos\left(\frac{a_1a_2+b^2}{[b^2(a_1^2+a_2^2+b^2)+a_1^2a_2^2]^{1/2}}\right)\right]+\pi \\ &\qquad (0\le\varphi\le 2\pi). \end{aligned} \qquad (39)$$

Fig. 4 provides a graphical representation of the phase-flux dependence based on our analytical approximation. This approach was accompanied by numerical simulations exploiting the program PSCAN [20], [21] (Fig. 5). A comparison of Figs. 4 and 5 shows that even for $l = 1$, where the analytical approximation is no longer valid, results are quite similar to those of the numerical simulation. The main conclusion from these figures is that there is nearly no phase shift for all φ, except in a tiny region around $\varphi = 2\pi$ where phase shift rapidly grows to 2π.

For very strong coupling, it is possible to derive a simple rule of thumb for the width of the small region around $\varphi = \pi$. For this purpose, we rewrite the phase shift as

$$\delta(\varphi) = \arctan(a_2/b) - \arctan(a_1/b), \quad 0 \le \varphi \le \pi. \qquad (40)$$

For $l \to 0$ the second arctan goes to $\frac{\pi}{2}$, whereas the first one changes its sign at the flux $\varphi^\star$,

$$\cos\frac{\varphi^\star}{2} - \frac{l}{2}\zeta_0\sin\frac{\varphi^\star}{2} = 0. \qquad (41)$$

Neglecting higher orders with respect to l, we obtain

$$\varphi^\star \simeq \pi - i_0 l. \qquad (42)$$

This provides a simple approximation for the phase of the cells under investigation,

$$\delta \simeq \pi\Theta(\varphi - \varphi^\star) \qquad (\varphi \le \pi). \qquad (43)$$

Fig. 6 confirms that for sufficiently small l the solution is indeed perfectly approximated by a Heaviside step function. This approximation might be useful considering more complicated arrays.

C. Remarks

Real junctions never have identical parameters. The response to parameter differences becomes particularly important in large arrays; here we consider junctions having different critical currents as well as normal resistances,

$$I_{c_1} \ne I_{c_2}, \quad R_{n_1} \ne R_{n_2}, \qquad (44)$$

under the subsidiary condition

$$I_{c_1}R_{n_1} = I_{c_2}R_{n_2} \qquad (45)$$

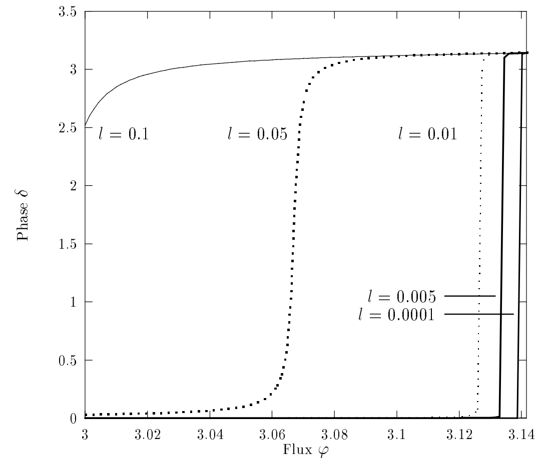

Fig. 6. Phase shift $\delta(\varphi)$ in the vicinity of $\varphi = \pi$ for extremely strong coupling, obtained from analytical approximation (39) ($i_0 = 1.5$).

which is usually satisfied with a good accuracy as a consequence of the technological process.

Introducing the mean critical current

$$I_c = \frac{1}{2}(I_{c_1} + I_{c_2}) \tag{46}$$

and the parameter splitting

$$\vartheta = (I_{c_2} - I_{c_1})/(I_{c_2} + I_{c_1}), \tag{47}$$

we derive the following modified equations of motion (cf. (21,22)) for the cell shown in Fig. 2:

$$\dot{\Sigma} + \sin\Sigma\cos\Delta = \frac{1}{1-\vartheta^2}i_0 - \frac{\vartheta}{l(1-\vartheta^2)}(\varphi - 2\Delta), \tag{48}$$

$$\dot{\Delta} + \cos\Sigma\sin\Delta = -\frac{\vartheta}{1-\vartheta^2}i_0 + \frac{1}{l(1-\vartheta^2)}(\varphi - 2\Delta). \tag{49}$$

This pair of equations already displays some effects qualitatively: (i) Up to the first order in ϑ there is a correction of the magnetic flux $\sim -i_0 l\vartheta$. (ii) There is a correction of the bias current $\vartheta(\varphi - 2\Delta)/l$ being of first order, too.

Treating loop inductance as well as parameter splitting as small expansion parameters,

$$\Sigma = \Sigma_0 + l\Sigma_{10} + \vartheta\Sigma_{01} + \cdots, \tag{50}$$

$$\Delta = \Delta_0 + l\Delta_{10} + \vartheta\Delta_{01} + \cdots, \tag{51}$$

we now can perform a perturbative treatment of the system (48,49) with respect not only to $l \ll 1$ but also to $\vartheta \ll 1$. Thus, as a result one finds that the Fourier coefficients $a_{1,2}$ (37) are unaffected by small parameter splittings ϑ, whereas there is an additional contribution to $b_{1,2}$,

$$b^{\vartheta}_{1,2} = b^{\vartheta} = 2\vartheta(i_0 + \cos\frac{\varphi}{2})\frac{\sin\frac{\varphi}{2}}{i_0 + \zeta_0}. \tag{52}$$

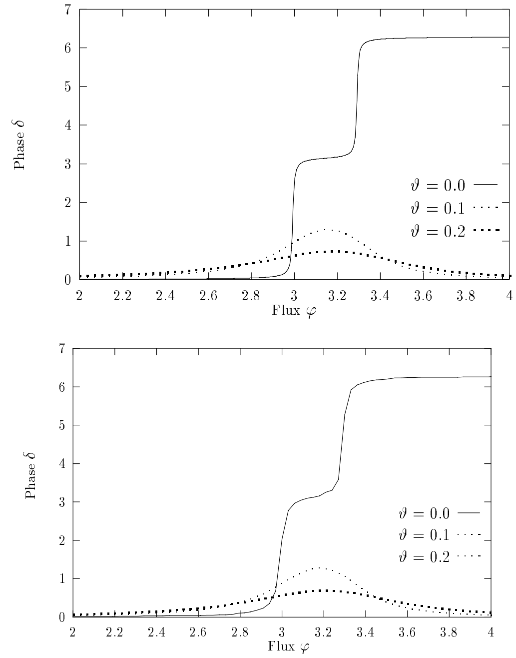

Fig. 7. The influence of parameter splitting ϑ on the phase shift $\delta(\varphi)$ for strong coupling obtained from analytical approximation (at the top) and numerical simulation (at the bottom); $i_0 = 1.5$, $l = 0.1$.

The phase shift $\delta(\varphi)$ obtained this way proves a conjecture on the dominant role of the loop inductance in the strong-coupling case (Fig. 7). One observes that the phase shift, being slightly raised generally, is considerably lowered for $\varphi \simeq \pi$.

III. Antiphase locking in a double cell

There may be several reasons responsible for poor radiation output generated by 2D Josephson junction arrays (cf. Sec. I). Besides technological problems this can as well result from the fact that basic mechanisms of phase locking in 2D networks, despite some interesting results on several aspects [7], [9], [22], [23], do not yet seem to be fully worked out theoretically. It is well known, though, that there is no phase locking in unshunted 2D arrays (without symmetry breaking architectures [17]) in absence of external flux. A theoretical study of the influence of a magnetic field using a "master slave mechanism" [22] led to the conclusion that an external flux can indeed lead to a certain phase locking; however, the definite value of the phase difference could not be determined, and stability was not considered at all.

Let us start here with a simple model configuration [24], consisting of two loops coupled via a line transverse to the bias current (Fig. 8). Despite of its simplicity it is difficult enough to show essential features of larger arrays. It is truly 2D with a possible flux entering the loops and an inductance in the transverse line, as is typically of hybrid arrays.

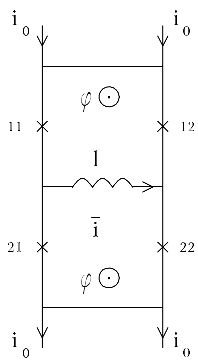

Fig. 8. The Josephson junction double cell with inductive coupling line.

A. Model of the double cell

Our propositions are as follows (cf. Fig. 8): (i) All junctions are considered to be identical. (ii) Self-inductance is taken into account while mutual inductances are neglected. (iii) There is no external load. (iv) We exploit a phase slip technique which has been applied successfully to 1D arrays before [10], [25], [26]. Their applicability crucially depends on the assumption that the normalized ring inductance is sufficiently small, $l \ll 1$. The dynamics of the junctions is described by the RSJ equations for the Josephson phases Φ_{ij},

$$\dot{\Phi}_{ij} + \sin\Phi_{ij} = i_{ij} \quad (i,j = 1,2), \tag{53}$$

completed by two flux quantization conditions,

$$\Phi_{12} - \Phi_{11} - \varphi - l\bar{i} = 0, \tag{54}$$
$$\Phi_{22} - \Phi_{21} - \varphi + l\bar{i} = 0. \tag{55}$$

In the following the transverse current playing a crucial role in the coupling is denoted by $\bar{i}$ (see Fig. 8). In addition, defining the circular currents,

$$i_i^\circ = (i_{i2} - i_{i1})/2 \quad (i = 1,2), \tag{56}$$

$\bar{i}$ can be expressed as

$$\bar{i} = i_2^\circ - i_1^\circ. \tag{57}$$

In strong coupling problems of this type it is useful to introduce (in analogy to Sec. II.A) sum and difference variables,

$$\Sigma_i = \frac{1}{2}(\Phi_{i2} + \Phi_{i1}), \;\; \Delta_i = \frac{1}{2}(\Phi_{i1} - \Phi_{i2}). \tag{58}$$

By the aid of these variables the problem (53-55) can be reformulated as

$$\dot{\Sigma}_i + \sin\Sigma_i \cos\Delta_i = i_0, \tag{59}$$
$$\dot{\Delta}_i + \cos\Sigma_i \sin\Delta_i = i_i^\circ, \tag{60}$$
$$\Delta_1 + \Delta_2 - \varphi = 0, \tag{61}$$
$$\Delta_1 - \Delta_2 - l(i_2^\circ - i_1^\circ) = 0. \tag{62}$$

This indicates that the voltage sums of both loops are controlled by the bias current $i_0 > 1$, while the circular currents control voltage differences. Eq. (61) is the flux quantization for the whole array, while Eq. (62) shows that differences in the circular currents spread the flux differences in the loops. The transverse current $\bar{i}$ can be obtained from

$$\bar{i} = i_2^\circ - i_1^\circ = \frac{1}{2}(\Delta_1 - \Delta_2). \tag{63}$$

B. Stable antiphase locking

The system (59-62) is treated perturbatively, assuming the ring inductance l to be sufficiently small:

$$\Sigma_i = \Sigma_{i,0} + l\Sigma_{i,1} + \cdots, \tag{64}$$
$$\Delta_i = \Delta_{i,0} + l\Delta_{i,1} + \cdots. \tag{65}$$

In the lowest order, flux quantization provides

$$\Delta_{i,0} = \frac{\varphi}{2},$$

i.e., junctions within both loops oscillate exactly in phase. The Josephson oscillation itself can be evaluated from Eq. (59) as

$$\Sigma_{i,0} = 2\arctan\left(\frac{\zeta_0}{i_0 + \cos\frac{\varphi}{2}} \tan\frac{\zeta_0 s - \delta_i}{2}\right) + \frac{\pi}{2}. \tag{66}$$

Using Eqs. (60), one determines the circular currents

$$i_i^\circ = \sin\frac{\varphi}{2}\cos\Sigma_{i,0} \tag{67}$$

with

$$\cos\Sigma_{i,0} = -\frac{\zeta_0 \sin(\zeta_o s - \delta_i)}{i_0 + \cos\frac{\varphi}{2}\cos(\zeta_0 s - \delta_i)}. \tag{68}$$

To summarize, in zero*th* order the junctions within each cell oscillate in phase independently of the value of the flux. However, the relative oscillation phase between the cells remains undetermined.

Passing to the next order, we start again from the Josephson phase differences (61-62) inserting the lowest order result (67). Finally, we get up to the first order

$$\Delta_{1,2} = \frac{\varphi}{2} \pm \sin\frac{\varphi}{2}\left(\cos\Sigma_{2,0} - \cos\Sigma_{1,0}\right). \tag{69}$$

From this result, one can read off the tranverse current

$$\bar{i} = \sin\frac{\varphi}{2}\left(\cos\Sigma_{2,0} - \cos\Sigma_{1,0}\right) \tag{70}$$

with the basic harmonic

$$\bar{i} = \frac{4\zeta_0 \sin\frac{\varphi}{2}}{i_0 + \zeta_0}\cos\left(\zeta_0 s - \frac{\delta_1 + \delta_2}{2}\right)\sin\left(\frac{\delta_2 - \delta_1}{2}\right). \tag{71}$$

We exploit the method of "slowly varying phase" for evaluating the Josephson phase sums of the cells. According to this method, first order corrections are put into the phases δ_i,

$$\delta_i = \delta_i(s), \tag{72}$$

which are supposed to change adiabatically in time (in comparison to the rf Josephson oscillations). In addition, we allow for the possibility that the joint synchronization frequency ζ be (slightly) different from the autonomous frequency ζ_0. With these assumptions the voltage sums can be written as

$$\dot{\Sigma}_i = \frac{\zeta_0(\zeta - \dot{\delta}_i)}{i_0 + \cos\frac{\varphi}{2}\cos(\zeta s - \delta_i)}. \tag{73}$$

Inserting this expression into Eq. (59) and neglecting higher orders in l, after some algebra we arrive at

$$\zeta_0(\zeta - \zeta_0 - \dot{\delta}_{1,2}) = \pm\frac{l}{4}\bar{i}(s)\sin\varphi \pm \frac{l}{2} i_0 \bar{i}(s)\sin\frac{\varphi}{2}\cos(\zeta s - \delta_{1,2}). \tag{74}$$

To proceed, we average over one oscillation period, considering δ_i as roughly constant over this time interval. It can be shown that only the lowest harmonic (70) of $\bar{i}$ contributes. The evaluation of mean values results in the evolution equations

$$\zeta_0(\zeta - \zeta_0 - \dot{\delta}_{1,2}) = \pm\frac{\zeta_0}{2(i_0+\zeta_0)}\sin^2\frac{\varphi}{2}\sin(\delta_1 - \delta_2). \tag{75}$$

Subtraction gives the so-called reduced equation for the phase difference $\delta_1 - \delta_2$,

$$\dot{\delta} = l\frac{i_0}{i_0+\zeta_0}\sin^2\frac{\varphi}{2}\sin\delta, \tag{76}$$

displaying formally the same structure as the RSJ equation describing an autonomous junction. It permits two phase-locking solutions,

$$\bar{\delta} = 0, \pi, \tag{77}$$

describing in-phase or antiphase oscillations of the cells. Investigation of stability leads to the Lyapunov coefficient

$$\lambda = l\frac{i_0}{i_0+\zeta_0}\sin^2\frac{\varphi}{2}\cos\bar{\delta}. \tag{78}$$

As a result, only antiphase oscillations are stable against small perturbations. To summarize, the following picture emerges: We know (cf. Sec. II), that the two junctions within each strongly coupled cell are generally (except for $\varphi \simeq \pi$) aligned in phase. In addition, both junctions of cell 1 oscillate in antiphase mode relative to those of cell 2. Synchronization of the cells in this state is provided by the alternating current $\bar{i}$, flowing through the joint transverse connection and playing the role of an order parameter. It is obvious that such a state will be nonradiating.

All results described analytically in this section are in complete agreement with corresponding numerical simulations. These show that the observed antiphase locking is not bound to the case of small inductances treated analytically here, but is a general feature of this type of arrays. If this remains true for larger arrays, which will be under investigation in the following sections, this might well explain the low radiation output obtained with 2D arrays up to now.

IV. Phase locking in Josephson ladder arrays

Here we study the phase locking in 2D arrays of the ladder type (cf. [27]). For this purpose, we exploit the specific formulation of the lowest harmonic approximation having proven useful in Sec. III in the study of double-cell arrays. As a result, we obtain conditions for the stability of the in-phase (or uniform) oscillation regime required for outcoupling the maximum radiation output from the array. Based on results of our previous investigations we focus on small-inductance cells guaranteeing a small phase shift within each cell. Thus the main question to be answered here concerns synchronization between cells in bias direction.

A. Josephson ladders: Basic conception

Fig. 9 shows the scheme of a ladder array of hybrid type with junctions only attached to the lines in bias direction [7]. We include the effect of non-vanishing external flux as well as non-vanishing inductances in longitudinal as well perpendicular direction relative to the bias direction. Moreover, we add an external shunt acting as a load via which the radiation may be outcoupled from the array. Based on the RSJ equations in conjunction with flux quantization within each loop and Kirchhoff's mesh rule for the external shunt loop we get the following system of equations descibing an N cell array with $i = 1, \cdots, N$ referring to cell i:

$$\dot{\Sigma}_i + \cos\Delta_i \sin\Sigma_i = i_0 - \frac{i_s}{2}, \tag{79}$$

$$\dot{\Delta}_i + \cos\Sigma_i \sin\Delta_i = i_i^\circ, \tag{80}$$

and

$$\Delta_i - \frac{\varphi}{2} + (l_\parallel + l_\perp) i_i^\circ - \frac{l_\perp}{2}(i_{i-1}^\circ + i_{i+1}^\circ) = 0, \tag{81}$$

$$\sum_{i=1}^{N}\ddot{\Sigma}_i - r_s\dot{i} - \lambda_s\ddot{i}_s - \frac{1}{c_s}i_s = 0. \tag{82}$$

Here we found it convenient to combine Josephson phases Φ_{i1}, Φ_{i2} within cell i as Σ_i, Δ_i according to rule (58); normalized circular currents are defined as $i_i^\circ = (I_{i2} - I_{i1})/2I_c$ (cf. (56)). In general, we have introduced scaled variables in agreement with guidelines in previous sections.

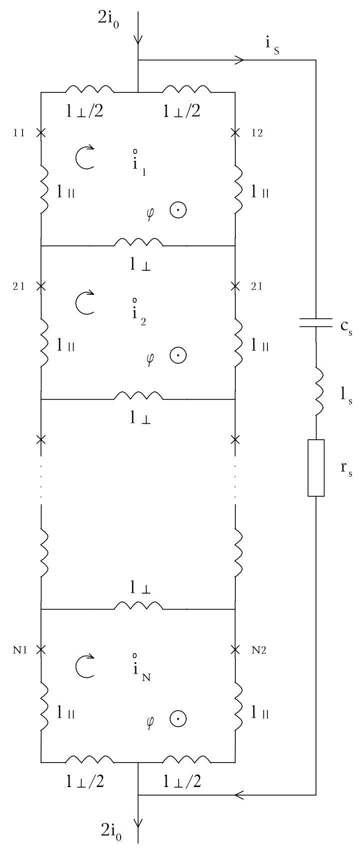

Fig. 9. The Josephson junction ladder array under consideration. $l_{\perp,\|}$ are the array's transverse and longitudinal inductances, while c_s, l_s, r_s refer to the external shunt's components. The shunt current flows as indicated through the load.

E.g., the shunt is characterized by the dimensionless capacitance $c_s = 2eR_n^2 I_c C_s/\hbar$, inductance $\lambda_s = 2\pi I_c(L_s + NL_\|/2 + L_\perp/2)/\Phi_0$ (where it is convenient to include the longitudinal inductances of the array as well) and resistance $r_s = R_s/R_n$ with C_s, L_s, R_s being the external shunt's capacitance, inductance, and resistance as being indicated in Fig. 9. All junctions are considered as being identical. The shunt is characterized by its impedance and phase angle as

$$z_s = \mid z_s \mid e^{i(\psi_s - \frac{\pi}{2})}, \tag{83}$$

where

$$\mid z_s \mid = \left[\left(r_s + \frac{N}{2} \right)^2 + \left(\lambda_s \zeta - \frac{1}{c_s \zeta} \right) \right]^{1/2}, \tag{84}$$

$$\sin \psi_s = \frac{r_s + N/2}{\mid z_s \mid}, \quad \cos \psi_s = \frac{1/c_s\zeta - \lambda_s \zeta}{\mid z_s \mid}. \tag{85}$$

B. Stable uniform phase locking

The normalized frequency ζ contained in the expressions (84,85) relates already to synchronization within the total ladder configuration. Indeed, applying the perturbative scheme including the method of slowly varying phase (along the lines developed in Sec. III) to the equations of motion (79-82) step by step, we arrive at the reduced equations

$$\begin{aligned} \dot{\delta}_i &= \zeta - \zeta_0 \\ &+ \frac{l_\perp}{2} \frac{i_0}{i_0 + \zeta_0} \sin^2 \frac{\varphi}{2} [\sin(\delta_i - \delta_{i+1}) + \sin(\delta_i - \delta_{i-1})] \\ &+ \frac{1}{i_0 + \zeta_0} \cos^2 \frac{\varphi}{2} \sum_{j=1}^{N} \sin(\delta_i - \delta_j - \psi_s), \\ &\qquad (i = 2, \cdots, N-1). \end{aligned} \tag{86}$$

Similar equations apply to the boundary cells.

The three terms in Eq. (86) admit of a clear interpretation. The first one is independent of the index i and leads to a frequency correction and as such will not be of interest in our context. The second characterizes the effect of internal interactions within the array, while the third one describes the long-range synchronizing effect of the external shunt. The contrary flux dependence of these two terms has remarkable consequences: For vanishing or nearly vanishing external flux, synchronization of the cells is completely controlled by the external shunt. However, for fluxes in the vicinity of π (corresponding to half a flux quantum per cell) the external shunt no longer has any effect. In this case the behavior of the array is controlled by its internal properties.

Next we combine phases δ_i as

$$\vartheta_i = \delta_{i+1} - \delta_i \quad (i = 1, \cdots, N-1).$$

This way we obtain reduced equations for the phase differences ϑ_i,

$$\begin{aligned} \dot{\vartheta}_i = &-\frac{l_\perp}{2} \frac{i_0}{i_0 + \zeta_0} \sin^2 \frac{\varphi}{2} (\sin \vartheta_{i+1} - 2 \sin \vartheta_i + \sin \vartheta_{i-1}) \\ &+ \frac{1}{\mid z_s \mid} \frac{1}{i_0 + \zeta_0} \cos^2 \frac{\varphi}{2} \left[\cos \left(\frac{\delta_{i+1} + \delta_i}{2} - \psi_s \right) \times \right. \\ &\times \sin \frac{\vartheta_i}{2} \sum_{j=1}^{N} \cos \delta_j \\ &\left. + \sin \left(\frac{\delta_{i+1} + \delta_i}{2} - \psi_s \right) \cos \frac{\vartheta_i}{2} \sum_{j=1}^{N} \sin \delta_j \right]. \end{aligned} \tag{87}$$

While we are unable to derive a general solution of this set of equations here, two important modes can be shown to exist. (For more detailed investigations see Sec. VI.) Simple inspection of (87) reveals the existence of the in-phase mode with

$$\vartheta_i = \delta_i = 0. \tag{88}$$

Closer inspection shows that at least for even N there also exists an antiphase mode with

$$\vartheta_i = \pi. \tag{89}$$

In the following, we concentrate on the stability of the maximally radiating in-phase mode (88). Based on the Lyapunov ansatz

$$\vartheta_i = 0 + \epsilon_i e^{\lambda s}, \qquad | \epsilon_i | \ll 1, \tag{90}$$

we arrive, via the conventional condition for nontrivial perturbation amplitudes, at $N-1$ Lyapunov exponents,

$$\lambda_k = \left(1 - \cos\frac{k\pi}{N}\right)\frac{l_\perp}{2}\sin^2\frac{\varphi}{2} + \frac{N\cos\psi_s}{4i_0 \mid z_s \mid}\cos^2\frac{\varphi}{2}$$
$$(k = 1, \cdots, n-1), \tag{91}$$

corresponding to $N-1$ possible relative oscillation modes.

Eq. (91) represents the main result of the stability considerations. The largest of the Lyapunov exponents limits the stability of the uniform oscillation mode of junctions adjacent in bias direction. The first term is positive, resulting from the fact that internal interaction attempts to destabilize this mode. However, as the sign of the second term depends on the character of the external load, this tendency can be overcome by adding an inductively dominated external shunt. Stable in-phase oscillations require ladders with (i) small inductances (ii) being shunted by an inductive external load.

It should be point outed that the coupling mechanism between the cells is qualitatively different from the one within cells: Within cells we have a SQUID-type coupling (cf. Sec. II) resulting in a flux-dependent continuous transition between the in-phase and the antiphase regime (becoming more abrupt the smaller the inductance is). On the other hand, coupling between cells is governed by a competition between long-range interaction controlled by the external load and short-range interaction controlled by the high-frequency currents flowing through the horizontal lines. While we did not cover all possible oscillation regimes, the result (91) indicates a flux-dependent point where the in-phase regime becomes instable.

V. Interaction of coupled interferometers

Thus we have seen that magnetic fields can influence the phase locking within a 2D array [11], [12] and consequently reduce the maximum output of oscillation power. In order to find a well-suited approach to the dynamics of general hybrid-type networks (Fig. 1), let us now study the problems, connected with external flux, of a $2 \times M$ array consisting of two rows (or interferometers), each of them with M junctions (Fig. 10). Repeatedly, the analysis is carried out by means of the small inductance perturbation scheme already successfully used (Secs. II-IV). For the sake of simplicity, both identical junctions (with vanishing capacitances) and identical cell inductances are presupposed. Without essential loss of generality we assume an even number M of junctions within the interferometers. This way we are able to replace the earlier

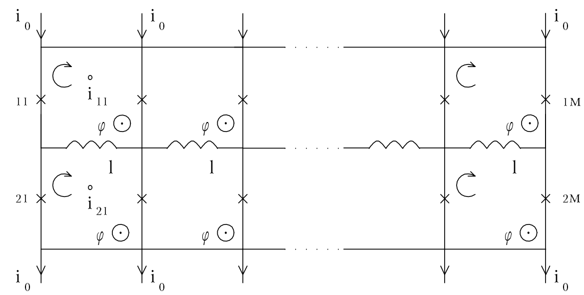

Fig. 10. The hybrid $2 \times M$ Josephson network consisting of two coupled interferometers.

definitions of sum and difference variables (cf. e.g. (58)) by the convenient pairing scheme [28], [29]

$$\Sigma_{kj} = (\Phi_{kM-j+1} + \Phi_{kj})/2,$$
$$\Delta_{kj} = (\Phi_{kM-j+1} - \Phi_{kj})/2 \tag{92}$$

for the original Josephson variables $\Phi_{kj}, \Phi_{kM-j+1}(k = 1, 2; j = 1, \cdots, \frac{M}{2})$.

A. Equations of motion and perturbation treatment

The dynamics of the double interferometer under consideration (Fig. 10) is described by the equations of motion,

$$\dot{\Sigma}_{kj} + \sin\Sigma_{kj}\cos\Delta_{kj} = i_0 + \frac{1}{2}\left(i^\circ_{k+1j-1} - i^\circ_{k+1j} + i^\circ_{k+1M-j} - i^\circ_{k+1M-j+1}\right) + l^{-1}\left(\Sigma_{kj-1} - 2\Sigma_{kj} + \Sigma_{kj+1}\right) \tag{93}$$

and

$$\dot{\Delta}_{kj} + \sin\Delta_{kj}\cos\Sigma_{kj} = i_0 + \frac{1}{2}\left(i^\circ_{k+1M-j} - i^\circ_{k+1M-j+1} + i^\circ_{k+1j-1} - i^\circ_{k+1j}\right) + l^{-1}\left(\Delta_{kj-1} - 2\Sigma_{kj} + \Delta_{kj+1}\right), \tag{94}$$

where the loop currents i°_{kj} have to satisfy the convention $i^\circ_{k0} = i^\circ_{kM} = 0$. Furthermore, we have introduced dummy variables,

$$\Sigma_{k0} = \Sigma_{k1}, \qquad \Sigma_{k\frac{M}{2}+1} = \Sigma_{k\frac{M}{2}},$$
$$\Delta_{k0} = \Delta_{k1} + \varphi, \qquad \Delta_{k\frac{M}{2}+1} = -\Delta_{k\frac{M}{2}},$$

and the rule that $k+1 \equiv 1$ applies to $k = 2$. In addition, we have to consider the flux quantization condition

$$\Phi_{kj-1} - \Phi_{kj} + \varphi + l\left(i^\circ_{k+1j-1} - i^\circ_{kj-1}\right) = 0$$
$$(k = 1, 2; j = 2, \cdots, M). \tag{95}$$

Now using the straightforward expansion procedure with respect to the small normalized inductance, $l \ll 1$,

$$\Sigma_{kj} = \Sigma_{kj,0} + l\Sigma_{kj,1} + \cdots, \tag{96}$$
$$\Delta_{kj} = \Delta_{kj,0} + l\Delta_{kj,1} + \cdots, \tag{97}$$

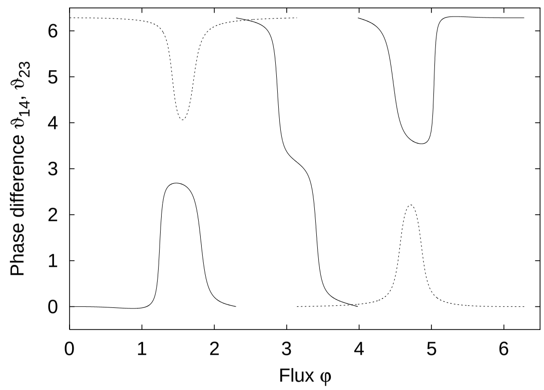

Fig. 11. Simple four-junction interferometer ($N=1, M=4$). Phase shift between the voltage oscillations of outer junctions, ϑ_{14} ($k=1$ and $k=4$, solid line), and inner junctions, ϑ_{23} ($k=2$ and $k=3$, dashed line); $l=0.1$, $i_0=1.5$.

we find the zero*th*-order solution

$$\Sigma_{kj,0} \equiv \Sigma_{k,0} \qquad (j=1,\cdots,\frac{M}{2}), \tag{98}$$

$$\Delta_{k\frac{M}{2}-j,0} = (2j+1)\frac{\varphi}{2} \quad (j=0,\cdots,\frac{M}{2}-1). \tag{99}$$

$\Sigma_{k,0}$ obeys the interferometer equation,

$$\dot{\Sigma}_{k,0} + c(\varphi)\sin\Sigma_{k,0} = i_0, \tag{100}$$

which contains the scaled critical interferometer current,

$$c(\varphi) = \frac{1}{M}\frac{\sin M\frac{\varphi}{2}}{\sin\frac{\varphi}{2}} \tag{101}$$

stipulating the autonomous frequency

$$\zeta_0 = (i_0 - c^2)^{1/2}. \tag{102}$$

Next, we determine the first-order circular currents by means of the approximated equations of motion,

$$i^{\circ}_{kj,0} = \sum_{\alpha=1}^{j}[c_{k,0}(\alpha) - s_{k,0}(\alpha)] \quad (1 \le j \le \frac{M}{2}), \tag{103}$$

$$i^{\circ}_{kM-j,0} = \sum_{\alpha=1}^{\frac{M}{2}}[c_{k,0}(\alpha) - s_{k,0}(\alpha)] - \sum_{\alpha=\frac{M}{2}}^{j+1}[c_{k,0}(\alpha)+s_{k,0}(\alpha)] \ \ (0 \le j \le \frac{M}{2}-1), \tag{104}$$

using the abbreviations

$$s_{k,0}(\alpha) = \sin\Sigma_{k,0}(\cos[(M+1-2\alpha)\frac{\varphi}{2}] - c(\varphi)),$$

$$c_{k,0}(\alpha) = \cos\Sigma_{k,0}\sin[(M+1-2\alpha)\frac{\varphi}{2}].$$

Here the trigonometric expressions have to be evaluated solving the interferometer equation (100) (cf. (66,68).

It is interesting to investigate the phase locking of the junctions within each interferometer, forgetting the inductive coupling between both rows for the moment. The mutual oscillation phase difference ϑ_{ik} of the ith and kth junction can be determined along the lines given in Sec. II.B. This phase shift as a function of external flux is shown in Fig. 11 for selected combinations i,k of a four-junction interferometer. It can be seen that for small inductances, $l \ll 1$, only a tiny phase shift between voltage oscillations exists unless the flux is close to multiples of $\Phi_0/4$. These points correspond to the zeros of the effective critical interferometer current $c(\varphi)$, cf. (101), and should be avoided for the realization of a synchronization regime. For larger interferometers the distance between the zeros at $2\pi/M$ becomes smaller with increasing number of M [30].

B. Stable mutual phase locking of both interferometers

To investigate the mutual phase locking of the interferometers, we have to develop a coupling scheme for both junction rows. It is reasonable to restrict the following considerations to the above-mentioned well-suited ranges avoiding the zeros of the critical interferometer current $c(\varphi)$.

First, recalling the mesh rule (95), we calculate the variables Δ_{kj} up to the first order with respect to $l \ll 1$,

$$\Delta_{kj} = \frac{M+1-2j}{2} - \frac{l}{2}\sum_{i=j}^{M-j}(i^{\circ}_{ki,0} - i^{\circ}_{k+1i,0}), \tag{105}$$

which can be completed by inserting the zero*th*-order ring currents (103,104). Second, we establish the slowly varying phases δ_k in the traditional manner (cf. (73)),

$$\dot{\Sigma}_k = \frac{\zeta_0(\zeta - \dot{\delta}_k)}{i_0 + c(\varphi)\cos(\zeta s - \delta_k)}, \tag{106}$$

and expand the cos term,

$$\cos\Delta_{kj} \simeq \cos[(M+1-2j)\frac{\varphi}{2}]$$

$$+\frac{l}{2}\sin[(M+1-2j)\frac{\varphi}{2}]\sum_{i=j}^{M-j}(i^{\circ}_{ki,0} - i^{\circ}_{k+1i,0}).[5mm] \tag{107}$$

Inserting these expressions into Eq. (93) and neglecting higher orders in l, after some algebra we arrive at

$$\zeta_0(\zeta - \zeta_0 - \dot{\delta}_k) =$$

$$= \frac{l}{M}[c(\varphi) + i_0\cos(\zeta s - \delta_k)]T(M,\varphi)\cos\Sigma_{k+1,0} \ \ (k=1,2). \tag{108}$$

Here, the complicated structure of the coupling parameter,

$$T(M,\varphi)=\left(\sum_{j=1}^{\frac{M}{2}}\sin[(M+1-2j)\frac{\varphi}{2}]\right)^2$$
$$+2\sum_{j=1}^{\frac{M}{2}-1}\sin[(M+1-2j)\frac{\varphi}{2}]\sum_{\alpha=j}^{\frac{M}{2}-1}\sum_{\beta=1}^{\alpha}\sin[(M+1-2\beta)\frac{\varphi}{2}], \tag{109}$$

reflects the complicated current distribution in the $2\times M$ network. Finally, averaging over one oscillation period $2\pi/\zeta$ and subtracting both Eqs. (108) gives the reduced equation for the phase difference $\delta=\delta_1-\delta_2$,

$$\dot{\delta}=l\frac{2i_0}{i_0+\zeta_0}\frac{T(M,\varphi)}{M}\sin\delta. \tag{110}$$

Generalizing the corresponding message of Sec. III, Eq. (110) admits of two phase-locking solutions,

$$\bar{\delta}=0,\pi, \tag{111}$$

whose stability is determined by the sign of the coupling strength $T(M,\varphi)$. Due to the leading first term, an inspection of expression (109) results in the statement

$$T(M,\varphi)\geq 0. \tag{112}$$

Immediately, one calculates for $M=2$ and $M=4$

$$T(2,\varphi)=\sin^2\frac{\varphi}{2}\geq 0$$

and

$$T(4,\varphi)=(\sin\frac{3\varphi}{2}+\sin\frac{\varphi}{2})^2+2\sin^2\frac{3\varphi}{2}\geq 0,$$

respectively. The result thus obtained is that only antiphase oscillations of both interferometers are stable.

VI. Phase locking dynamics of hybrid $N\times M$ Josephson junction arrays

We have already seen (Sec. IV) that the dynamic behavior of ladder arrays with small loop inductances is quite similar to that of 1D arrays, which have been known to require an inductive load for obtaining in-phase oscillations [10], [25]. Following this idea, we investigate now the synchronization of general $N\times M$ hybrid Josephson junction arrays by considering them as 1D chains of N interferometers (Fig. 1). Each interferometer row consists of M strongly coupled junctions and, therefore, it forms a homogeneous whole described by the coherent variable (cf. (106))

$$\dot{\Sigma}_k=\frac{\zeta_0(\zeta-\dot{\delta}_k)}{i_0+c(\varphi)\cos(\zeta s-\delta_k)}\quad (k=1,\cdots,N)$$

within the phase slip picture. Due to the positive sign of the coupling parameter (112), the interaction of adjacent rows causes their mutual antiphase locking. However, we try to overcome this tendency by adding an external inductive load to the Josephson network. Generalizing some basic ideas already exploited in Sec. IV, we express the arising competition between nearest-neighbour and long-range coupling by means of the following reduced equations for slowly varying phases,

$$\dot{\delta}_k=\zeta-\zeta_0+\beta[\sin(\delta_k-\delta_{k-1})+\sin(\delta_k-\delta_{k+1})]$$
$$+\gamma\sum_{j=1}^{N}\sin(\delta_k-\delta_j-\psi_s)\quad (k=2,\cdots,N-1), \tag{113}$$

with the parameters

$$\beta=\frac{l_\perp}{M}\frac{i_0}{i_0+\zeta_0}T(M,\varphi), \tag{114}$$

$$\gamma=\frac{1}{2\mid z_s\mid}\frac{1}{i_0+\zeta_0}c^2(\varphi). \tag{115}$$

Similar equations apply to the boundary interferometers $(k=1,N)$.

We note that the short-range coupling strength (114) contains the transverse cell inductance only, whereas its long-range counterpart (115) considers via the shunt impedance z_s all inductances being "felt" by the current flowing through the external loop. Furthermore, the condition for an inductively dominated load reads as

$$\cos\psi_s<0. \tag{116}$$

We must keep in mind that for larger interferometers the distance between the zeros of the critical current decreases with increasing number M of junctions (cf. Sec. V.A). Therefore, from an experimental point of view it is reasonable to confine the flux through the cell to small values,

$$\mid\varphi\mid<\frac{2\pi}{M}\ll 1. \tag{117}$$

This way an inspection of the coupling strength tells us that in this operation range its ratio

$$\mu=\frac{\beta}{\gamma}\ll 1$$

is small and may serve as expansion parameter of a perturbation procedure for determinig phase-locked (or stationary) solutions, $\delta_k=\bar{\delta}_k=$ const., of the system (113) being reformulated as

$$E=\mu[\sin(\bar{\delta}_k-\bar{\delta}_{k-1})+\sin(\bar{\delta}_k-\bar{\delta}_{k+1})]$$
$$+\sum_{j=1}^{N}\sin(\bar{\delta}_k-\bar{\delta}_j-\psi_s) \tag{118}$$

with

$$E=\gamma^{-1}(\zeta-\zeta_0) \tag{119}$$

describing the detuning of the interferometer frequency, $\zeta_0 = (i_0^2 - c^2(\varphi))^{1/2}$, and the network synchronization frequency, ζ. Inserting the expansion

$$\bar{\delta}_k = \bar{\delta}_{k,0} + \mu \bar{\delta}_{k,1}, \tag{120}$$

we find in zero*th* order the uniform mode (cf. [10], [25], [26], [31])

$$\bar{\delta}_{k,0} \equiv \bar{\delta}_0 \tag{121}$$

being stable in the inductive regime as is well-known for series arrays (116). The first-order corrections obey the equations

$$\cos\psi_s \sum_{j=1}^{N} (\bar{\delta}_{j,1} - \bar{\delta}_{k,1}) = 0 \tag{122}$$

permitting the solution

$$\bar{\delta}_{k,1} \equiv \bar{\delta}_1 \tag{123}$$

which provides the zero*th*-order solution merely with a shift,

$$\bar{\delta}_k = \bar{\delta}_0 + \mu \bar{\delta}_1, \tag{124}$$

i.e., the character of the uniform mode in the hybrid Josphson network is not affected by minor short-range interactions of adjacent interferometers.

Next, we have to check the stability of this coherent mode. Based on the Lyapunov ansatz

$$\delta_k = \delta_k(s) = \bar{\delta}_k + \epsilon_k e^{\lambda s}, \tag{125}$$

we derive the linear algebraic system

$$(\lambda - N\gamma\cos\psi_s - 2\mu\gamma)\vartheta_i + \mu\gamma(\vartheta_{i-1} + \vartheta_{i+1}) = 0 \tag{126}$$

for the relative perturbation amplitudes

$$\vartheta_k = \epsilon_{k+1} - \epsilon_k.$$

The system (126) allows non-trivial solutions only for the Lyapunov exponents

$$\lambda_k = N\gamma\cos\psi_s + 2\mu\gamma\left(1 + \cos\frac{k\pi}{N}\right)$$

$$(k = 1, \cdots, N-1). \tag{127}$$

The second term on the r.h.s. presents a perturbative contribution only. With a well defined inductive regime assumed,

$$\mid N\gamma\cos\psi_s \mid > 2\mu\gamma,$$

the network under consideration operates in a stable uniform mode.

VII. Summary and conclusions

We have discussed theoretically possibilites for the realization of mm and sub-mm wavelength radiation sources based on 2D discrete Josephson arrays. In particular, we have investigated the problem of phase locking in $N \times M$ hybrid Josephson networks with small loop inductances. Since the basic component of such special arrays is the SQUID-like cell, we have demonstrated the fact of a merely tiny phase shift between the voltage oscillations of both junctions. Otherwise, two loops coupled via a joint line transverse to the bias current oscillate in a stable antiphase regime. In order to generalize these results, we have considered the dynamics of $N \times 2$ ladders and $2 \times M$ multi-junction interferometers exploiting basic ideas about the interplay of strong and weak coupling transverse to bias direction and along the current biasing, respectively. In princple, the coupling within interferometers provides the possibility of nearly in-phase oscillations of all junctions in the row. On the other hand, coupling between adjacent interferometers tends to cause antiphase locking.

This way we found a simple approach to synchronization in general $N \times M$ hybrid arrays. Adding an inductively dominated load to the network, we have shown the existence of a uniform mode which is characterized by a perfect phase locking of all junctions in the array with a common oscillation phase. The configuration resembles a linear design of oscillators (consisting of strongly coupled interferometers here).

We note the incompleteness of our considerations due to missing fluctuation terms in the respective equations of motion. However, the crucial point is the external flux penetrating a loop. Near the zeros of the critical interferometer current the uniform mode is lost. This is a serious problem of large arrays with many columns because the distance between the zeros at Φ_0/M decreases with increasing number M of junctions per row. Therefore, the external flux has to be suppressed below Φ_0/M so that a synchronous regime can be maintained.

In principle, this could be achieved by applying a superconducting groundplane close to the array, which may result in effective shielding. However, it is crucial that no magnetic flux is trapped in the groundplane. Trapped flux may penatrate some of the loops; furthermore, certain jumps of localized flux may result in random noise. We hope that experimenters may soon overcome the mentioned difficulties in order to establish the possibility to realize effective (maximum power) radiation sources up to the THz-range by means of HT_c superconducting networks.

Acknowledgement

This publication is based on the presentations made at the European Research Conference (EURESCO) on “Future Perspectives of Superconducting Josephson De-

vices: Euroconference on Physics and Application of Multi-Junction Superconducting Josephson Devices", Acquafredda di Maratea, Italy, 1-6 July 2000, organized by the European Science Foundation and supported by the European Commission, Research DG, Human Potential Programme, High-Level Scientific Conferences, Contract HPCFCT-1999-00135.
This information is the sole responsibility of the authors and does not reflect the ESF's or the Community's opinion. The ESF and the Community are not responsible for any use that might be made of data appearing in this publication.

References

[1] J. B. Hansen and P. E. Lindelof, Rev. Mod. Phys. **56**, 431 (1986).
[2] J. E. Lukens, in: *Modern Superconducting Devices*, eds. S. T. Ruggiero and D. A. Rudman, Academic Press, New York 1990, pp. 135–167.
[3] M. Darula, T. Doderer, and S. Beuven, Supercond. Sci. Technol. **12**, R1 (1999).
[4] S. P. Benz and C. J. Burroughs, Supercond. Sci. Technol. **4**, 561 (1999).
[5] S. P. Benz and C. J. Burroughs, Appl. Phys. Lett. **58**, 2162 (1991).
[6] P. A. A. Booi and S. P. Benz, Appl. Phys. Lett. **68**, 3799 (1996).
[7] R. L. Kautz, IEEE Trans. Appl. Supercond. **5**, 2702 (1995).
[8] B. R. Trees and Stroud, Phys. Rev. B **59**, 7108 (1999).
[9] K.Wiesenfeld, S. P. Benz, and P. A. A. Booi, J. Appl. Phys. **76**, 3835 (1994).
[10] A. K. Jain, K. K. Likharev, J. E. Lukens, and J. E. Savageau, Phys. Rep. **109**, 310 (1984).
[11] P. A. A. Booi, *High-Frequency Array Oscillators Based on* $Nb/Al - AlO_x/Nb$ *Junctions*, Ph. D. Thesis, Twente University, 1995.
[12] S. G. Lachenmann, *Dynamik von Josephson-Kontakt-Netzwerken*, Ph. D. Thesis, Eberhard-Karls-Universität Tübingen, 1995.
[13] W. Krech and K. Yu. Platov, J. Appl. Phys. **77**, 1640 (1995).
[14] W. Krech, Wiss. Z. FSU Jena, Math.-Nat. R. **32**, 19 (1983).
[15] M. Basler, W. Krech, and K. Yu. Platov, in: *Macroscopic Quantum Phenomena and Coherence in Superconducting Networks*, eds. C. Giovanella and M. Tinkham, World Scientific, Singapore 1995, pp. 225–234.
[16] M. Keck, T. Doderer, R. Müller, R. Pfeifer, A. Laub, R. P. Huebener, T. Traeuble, R. Dolata, T. Weimann, and J. Niemeyer. IEEE Trans. Appl. Supercond. **7**, 3407 (1997).
[17] J. Oppenländer, W. Güttinger, T. Traeuble, M. Keck, T. Doderer, and R. P. Huebener, IEEE Trans. Appl. Supercond. **9**, 4337 (1999).
[18] S. Kiruyu, W. Zhang, S. Han, S. Deus, and J. E. Lukens, IEEE Trans. Appl. Supercond. **7**, 3107 (1997).
[19] M. Basler, W. Krech, and K. Yu. Platov, Phys. Rev. B **52**, 7504 (1995).
[20] A.A. Odintsov, V. K. Semenov, and A. B. Zorin, IEEE Trans. Magn. **23**, 763 (1987).
[21] V. K. Semenov, A. A. Odintsov, and A. B. Zorin, in: *SQUID'85*, eds. H. D. Hahlbohm and H. Lübbig, de Gruyter, Berlin 1985, pp. 71–75.
[22] G. Filatrella and K. Wiesenfeld, J. Appl. Phys. **78**, 1878 (1995).
[23] M. Darula, P. Seidel, F. Busse, and S. Benacka, J. Appl. Phys. **74**, 2674 (1993).
[24] M. Basler, W. Krech, and K. Yu. Platov, J. Appl. Phys. **80**, 3598 (1996).
[25] W. Krech, Ann. Phys. (Leipzig) **39**, 117 (1982).
[26] W. Krech, Ann. Phys. (Leipzig) **39**, 349 (1982).
[27] M. Basler, W. Krech, and K. Yu. Platov, Appl. Phys. Lett. **72**, 252 (1998).
[28] B. Frank, W. Krech, and K. Yu. Platov, J. Appl. Phys. **84**, 1476 (1998).
[29] B. Frank, M. Basler, W. Krech, K. Yu. Platov, and H.-G. Meyer, IEEE Trans. Appl. Supercond. **9**, 4550 (1999).
[30] K. K. Likharev, *Dynamics of Josephson junctions and circuits*, Gordon and Breach, Philadelphia 1991.
[31] H.-G. Meyer and W. Krech, J. Appl. Phys. **68**, 2868 (1990).